




Research Article

A Water-Soluble Hydrogen Sulfide Donor Suppresses the Growth of Hepatocellular Carcinoma via Inhibiting the AKT/GSK-3 β / β -Catenin and TGF- β /Smad2/3 Signaling Pathways

Shao-Feng Duan,^{1,2} Meng-Meng Zhang,¹ Qian Dong,¹ Bo Yang,¹ Wei Liu,¹ Xin Zhang,¹ Hai-Lan Yu,¹ Shi-Hui Zhang,¹ Nazeer Hussain Khan,³ Dong-Dong Wu ,³ Xiao-Ju Zhang ,⁴ and Juan Cen ⁵

¹School of Pharmacy, Henan University, Kaifeng, Henan 475004, China

²Henan International Joint Laboratory for Chinese Medicine Efficacy, Henan University, Kaifeng, Henan 475004, China

³Henan International Joint Laboratory for Nuclear Protein Regulation, School of Basic Medical Sciences, Henan University, Kaifeng, Henan 475004, China

⁴Department of Respiratory and Critical Care Medicine, Henan Provincial People's Hospital, Zhengzhou University People's Hospital, Zhengzhou, Henan 450003, China

⁵Key Laboratory of Natural Medicine and Immune Engineering, School of Pharmacy, Henan University, Kaifeng, Henan 475001, China

Correspondence should be addressed to Dong-Dong Wu; ddwubiomed2010@163.com, Xiao-Ju Zhang; 15837101166@163.com, and Juan Cen; cenjuan@vip.henu.edu.cn

Received 13 July 2022; Revised 1 February 2023; Accepted 10 February 2023; Published 7 March 2023

Academic Editor: Manu Kanjoormana Aryan

Copyright © 2023 Shao-Feng Duan et al. This is an open access article distributed under the Creative Commons Attribution License, which permits unrestricted use, distribution, and reproduction in any medium, provided the original work is properly cited.

Hepatocellular carcinoma (HCC) is a disease with high morbidity, high mortality, and low cure rate. Hyaluronic acid (HA) is widely adopted in tissue engineering and drug delivery. 5-(4-Hydroxyphenyl)-3H-1, 2-dithiol-3-thione (ADT-OH) is one of commonly used H₂S donors. In our previous study, HA-ADT was designed and synthesized via coupling of HA and ADT-OH. In this study, compared with sodium hydrosulfide (NaHS, a fast H₂S-releasing donor) and morpholin-4-ium (4-methoxyphenyl)-morpholin-4-ylsulfanylidene-sulfido- λ -5-phosphane (GYY4137, a slow H₂S-releasing donor), HA-ADT showed stronger inhibitory effect on the proliferation, migration, invasion, and cell cycle of human HCC cells. HA-ADT promoted apoptosis by suppressing the expressions of phospho (p)-protein kinase B (PKB/AKT), p-glycogen synthase kinase-3 β (GSK-3 β), p- β -catenin, and also inhibited autophagy via the downregulation of the protein levels of p-Smad2, p-Smad3, and transforming growth factor- β (TGF- β) in human HCC cells. Moreover, HA-ADT inhibited HCC xenograft tumor growth more effectively than both NaHS and GYY4137. Therefore, HA-ADT can suppress the growth of HCC cells by blocking the AKT/GSK-3 β / β -catenin and TGF- β /Smad2/3 signaling pathways. HA-ADT and its derivatives may be developed as promising antitumor drugs.

1. Introduction

Liver cancer is one of the leading causes of cancer death worldwide [1–4]. It is a heterogeneous, invasive, and drug-resistant malignant disease with poor prognosis [5–7], which is also the most common malignant tumor in the digestive system, with high mortality and low

survival rate [3, 8]. Infection with hepatitis viruses and dietary exposure to aflatoxin are the main causes of liver cancer [9]. Hepatocellular carcinoma (HCC) is a highly invasive and most common liver cancer [10–12]. Many factors can contribute to the development of liver cancer, including hepatitis B virus, hepatitis C virus, cirrhosis, alcoholism, obesity, poor diet and inactivity, and

mycotoxins [13–18]. Recent studies have shown undifferentiated liver cancer stem cells to be the main cause for the occurrence, metastasis, recurrence, and chemotherapy resistance of liver cancer [11, 19]. Liver cancer patients often die due to difficulties in early diagnosis, missed opportunity for surgical resection, and delayed treatment [3, 6]. Further research is urgent to advance the prevention, diagnosis, and treatment of liver cancer [13, 20].

Hydrogen sulfide (H_2S) is a water-soluble and colorless gas with the rotten egg odor [21, 22]. The physiological function of H_2S has been firstly demonstrated in the mammalian brain [23]. H_2S has been identified as a gaseous signaling molecule, and together with carbon monoxide (CO) and nitric oxide (NO), forms a bioactive gas transmitter group [24–28]. H_2S plays an important role in signal transduction in a variety of physiological and pathological processes [29–35]. Cystathionine γ -lyase (CSE), cystathionine β -synthetase (CBS), and 3-mercaptopyruvate sulfurtransferase (3-MST) are three main enzymes involved in endogenous H_2S biosynthesis under physiological conditions [21, 32, 36, 37]. H_2S breakdown is accomplished by a mitochondrial pathway that couples H_2S oxidation into sulfate and thiosulfate to adenosine triphosphate synthesis [32]. In addition to the absorption of H_2S through diffusion, a small amount of endogenous H_2S can also be produced by the dietary L-homocysteine through the sulfur transfer pathway. This process is mainly completed by two enzymes, CBS and CSE, which depend on pyridoxal-5'-phosphate. CBS and CSE use cystathionine to convert homocysteine into cysteine, and H_2S is a byproduct. In addition, 3-MST can also generate H_2S . It uses mercaptopyruvate to form persulphide intermediately through α -ketoglutarate and cysteine transaminase, and then release H_2S and pyruvate through reduction reaction [26, 29, 36, 38].

Hyaluronic acid (HA) is a glycosaminoglycan widely existing in human body. HA, a natural polysaccharide, is composed of N-acetylglucosamine and glucuronic acid, which are alternately linked by β -1, 3 and β -1, 4 glycoside bonds [39, 40]. Because HA and its derivatives have the characteristics of high viscoelasticity, plasticity, non-immunogenicity, good biocompatibility, degradation, and binding with specific receptors on the cell surface, they are often used as slow-release carriers of drugs or as active target ligands of modified nano carriers to achieve the thickening, slow-release, transdermal absorption of drugs and improve the targeting and bioavailability of drugs [39–41]. HA and drug conjugates have been shown to have the dual advantages of tumor site aggregation and receptor-mediated endocytosis [40]. 5-(4-hydroxyphenyl)-3H-1, 2-dithiol-3-thione (ADT-OH) is the most widely used agent in the synthesis of slow H_2S -releasing donors. ADT is a methyl derivative of ADT-OH, which can be metabolized by mitochondrial enzymes to produce H_2S [42, 43].

A number of studies have shown that the protein kinase B (PKB/AKT)/glycogen synthase kinase-3 β (GSK-3 β)/ β -catenin pathway plays an important role in the progression of liver cancer [44–46]. Furthermore, the transforming growth factor- β (TGF- β)/Smad2/3 pathway is involved in the proliferation,

migration, invasion, and epithelial-mesenchymal transition (EMT) of liver cancer [47–49]. Diallyl trisulfide, an H_2S donor, regulates cell invasion and apoptosis via the phosphatidylinositol 3-kinase/AKT/GSK-3 β signaling pathway in human osteosarcoma U2OS cells [50]. Another study indicates that H_2S can attenuate paraquat-induced EMT of human alveolar epithelial cells by regulating the TGF- β 1/Smad2/3 pathway [51]. Our previous study has demonstrated that H_2S plays a double-edged sword role in human HCC cells, suggesting that novel H_2S donors can be designed and applied for the treatment of cancer [52].

In this study, a new coupling compound HA-ADT was designed and synthesized as previously described [53]. HA-ADT could generate more H_2S than both sodium hydrosulfide (NaHS, a fast H_2S -releasing donor) and morpholin-4-ium (4-methoxyphenyl)-morpholin-4-ylsulfanylidene-sulfido- λ 5-phosphane (GY4137, a slow H_2S -releasing donor) [53]. The roles of HA-ADT in the proliferation, migration, and invasion of human HCC cells were investigated. Then we conducted *in vivo* experiments to further determine the effect of HA-ADT on the growth of human HCC xenografts.

2. Materials and Methods

2.1. Cell Culture. Human HCC cell lines SMMC-7721 and Huh-7 were obtained from Kebai Biological Technology Co., Ltd. (Nanjing, Jiangsu, China). SMMC-7721 cells were grown in RPMI1640 medium supplemented with 10% fetal bovine serum (FBS), penicillin (100 U/ml), and streptomycin (100 μ g/ml). Huh-7 cells were grown in DMEM supplemented with 10% FBS, penicillin (100 U/ml), and streptomycin (100 μ g/ml). Cells were cultured in an incubator at 37°C with 95% air and 5% CO₂. Cells were treated with NaHS (200 μ M), GY4137 (200 μ M), and HA-ADT (200 μ M) (provided by Prof. Shao-Feng Duan), respectively [53]. The control group was treated with phosphate-buffered saline (PBS). After treatment for 24 h, the cells were adopted for following experiments.

2.2. Cell Growth Assay. The Cell-Light 5-ethynyl-2-deoxyuridine (EdU) Apollo 567 Kits (RiboBio, Guangzhou, China) were used to detect cell proliferation. Cell proliferation rate = (EdU-positive cells)/(total cells) \times 100% [54]. The 3-(4, 5-dimethyl-2-thiazolyl)-2, 5-diphenyl-2-H-tetrazolium bromide (MTT) (Sigma, St. Louis, MO, USA) and CCK-8 detection kits (Beyotime, Shanghai, China) were adopted to determine cell viability [55–57].

2.3. Colony Formation Assay. The cells (1×10^3 per well) were cultivated in a culture medium for 2 weeks at 37°C. After washing with PBS, the colonies were fixed with methanol. Crystal violet was then added and incubated at room temperature for 30 min. The plates were washed, air-dried, and scanned. Then, the colony number was counted.

2.4. Wound Healing Assay. The cultured monolayer-confluent cells were scratched. The migration distance was photographed under an inverted microscope (Olympus

CKX41, Tokyo, Japan). The cell migration rate (MR) was calculated as $MR (\%) = [(A - B)/A] \times 100$, where A and B are the widths at 0 h and 24 h, respectively [58].

2.5. Migration and Invasion Assays. The cells (1×10^5) were seeded into the matrigel coated/uncoated upper chamber. The medium supplemented with 20% FBS was added into the lower chamber. After 24 h of treatment, the remaining cells on the upper side were scrubbed off, and the cells on the bottom side were fixed with 4% paraformaldehyde, and then stained with 0.1% crystal violet for 20 min. The cells were counted using an Axioskop 2 plus microscope (Zeiss, Thornwood, NY, USA).

2.6. Flow Cytometry Analysis. 1×10^6 cells were trypsinized and then fixed in ice-cold 75% ethanol overnight. After washing with PBS, the cells were incubated in propidium iodide (PI)/RNase A mixture at room temperature for 30 min. The cell cycle distribution was analyzed with a FACSVerser flow cytometer (CytoFLEX S, Beckman, CA, USA). The apoptotic level was detected using the Annexin V and PI apoptosis kits (UE, Suzhou, Jiangsu, China) and analyzed using a FACSVerser flow cytometer.

2.7. TdT-Mediated dUTP-Biotin Nick End Labeling (TUNEL) Assay. TUNEL assay was carried out using the *in situ* cell death detection kits (Beyotime). The cells were examined with a fluorescence microscope (Nikon Eclipse Ti, Melville, NY, USA). The percentage of TUNEL positive cells was further quantified.

2.8. Western Blotting. Total protein was extracted from human HCC cells. Western blotting was used to determine the expression levels of relevant proteins. The primary antibodies include anti-Cyclin E1, anti-Cyclin D1, anti-cyclin-dependent kinase (CDK) 2, anti-CDK4, anti-p27, anti-p21, anti-AKT, anti-phospho (p)-AKT (Ser473), anti-glycogen synthase kinase-3 beta (Gsk-3 β), anti-p-Gsk-3 β (Ser9), anti- β -catenin, anti-p- β -catenin (Ser552), anti-beclin-1, anti-p62, anti-LC3A/B, anti-Smad2, anti-p-Smad2 (Ser465/467), anti-Smad3, anti-p-Smad3 (Ser423/425), and anti-transforming growth factor-beta (TGF- β) antibodies, as well as the horseradish peroxidase-conjugated secondary antibody obtained from Cell Signaling Technology (CST, Danvers, MA, USA). Anti-B-cell lymphoma-2 (Bcl-2), anti-B-cell lymphoma-extra large (Bcl-xl), anti-Bcl-2-associated X protein (Bax), anti-Bcl-xl/Bcl-2-associated death promoter (Bad), anti-cleaved caspase (cas)-3, anti-cleaved cas-9, anti-cleaved poly adenosine diphosphate-ribose polymerase (PARP), and anti- β -actin antibodies were obtained from ProteinTech (Chicago, IL, USA). The protein bands were detected with the enhanced chemiluminescence system (Thermo, Rockford, IL, USA) and semiquantified by ImageJ software.

2.9. Animal Study. Animal experiments were approved by the Committee of Medical Ethics and Welfare for Experimental Animals of Henan University School of Medicine

(HUSOM-2017-218). Animal study was carried out as previously described [53]. BALB/c nude mice (male, 4-week-old) were obtained from Vital River Laboratory Animal Technology Co., Ltd. (Beijing, China). 5×10^6 SMMC-7721/Huh-7 cells in PBS (200 μ L) were injected subcutaneously into the right flank of each mouse. The mice were divided randomly into 4 groups ($n = 6$ per group). NaHS (200 μ M), GYY4137 (200 μ M), HA-ADT (200 μ M), and PBS were administered subcutaneously once-a-day for 21 days. During the animal experiment, the mice were daily weighed. The tumor volume was calculated as follows: Volume (V) = $1/2 \times W^2 \times L$, where L and W are the longest and widest dimension, respectively [59]. The tumor volume doubling time (TVDT) was calculated as follows: $TVDT = (T - T_0) \times \log 2 / \log (V_2/V_1)$, where V_2 and V_1 are the tumor volume at two measurement times and $(T - T_0)$ is the time interval [60, 61]. At the end of the experiment, all mice were sacrificed. Then the tumors were excised, weighted, and photographed. Inhibition rate (IR) = $[(A - B)/A] \times 100\%$, where A and B are the average tumor weight of control group and the treatment group, respectively [53].

2.10. Hematoxylin and Eosin (HE) Staining. Tumor tissues were fixed in 10% neutral-buffered formalin, embedded in paraffin, sectioned at 5 μ m thickness, and then stained with HE. The tissues were observed using a Zeiss Axioskop 2 plus microscope.

2.11. Immunohistochemistry (IHC). Microvessel density (MVD) has been widely used as an index for the angiogenic activity [62]. The proliferation index (PI) was calculated as the percentage of Ki67-positive cells to total cells [63]. Apoptotic index was determined as cleaved cas-3 -positive cells to total cells [64]. Tumor tissues were stained with anti-CD31 (CST), anti-Ki67 (CST), anti-p21, anti-cleaved cas-3, and anti-beclin-1 antibodies, respectively. The proliferation index (PI), apoptosis index, MVD, p21-positive cells, and autophagy index were counted according to the ratio of positive cells to total cells.

2.12. Statistical Analysis. All results are expressed as the mean \pm standard error of the mean (SEM). Differences among groups were determined using one-way analysis of variance with SPSS 19.0 software, followed by Tukey's test. A P value of less than 0.05 was considered statistically significant.

3. Results

3.1. HA-ADT Inhibits the Growth, Migration, and Invasion of Human HCC Cells. Compared with the control, NaHS, and GYY4137 group, HA-ADT significantly suppressed the viability and proliferation of Huh-7 and SMMC-7721 cells (Figures 1(a)–1(e)). HA-ADT also more effectively reduced the colony formation of SMMC-7721 and Huh-7 cells (Figures 1(f) and 1(g)). In addition, HA-ADT showed more inhibitory effects on the migration and invasion of Huh-7

and SMMC-7721 cells than the control, NaHS, and GYY4137 group (Figure 2). In summary, the results show that HA-ADT could inhibit the growth, migration, and invasion of HCC cells.

3.2. HA-ADT Blocks Cell Cycle of Human HCC Cells. As shown in Figures 3(a) and 3(b), HA-ADT significantly upregulated the percentage of cells in S phase but downregulated the percentage of cells in G2 phase, suggesting that HA-ADT blocked the cell cycle in S phase. Western blot was further conducted to detect the protein levels of cyclin D1/E1, CDK2/4, p21, and p27. The results indicated that HA-ADT decreased the levels of cyclin D1/E1 and CDK2/4, but increased the levels of both p21 and p27 (Figures 3(c) and 3(d)). These results indicate that HA-ADT can block the cell cycle of human HCC cells at S phase by regulating the expression levels of cell cycle-related proteins.

3.3. HA-ADT Promotes Apoptosis by Suppressing the AKT/GSK-3 β / β -Catenin Signaling Pathway in Human HCC Cells. Apoptosis was detected by TUNEL and flow cytometry assays. As shown in Figures 4(a)–4(d), the apoptotic level in the HA-ADT group was significantly increased when compared with the control, NaHS, and GYY4137 group. The ratios of Bax/Bcl-2 and Bad/Bcl-xl are important indicators of apoptosis. Increased Bax/Bcl-2 and Bad/Bcl-xl ratios have been found in mitochondria-mediated apoptosis [65, 66]. As shown in Figure S1, Bax/Bcl-2 and Bad/Bcl-xl ratios in the HA-ADT group were obviously increased. In addition, the expression levels of cleaved cas-3, 9, and cleaved PARP exhibited similar trends. The AKT/GSK-3 β / β -catenin cascade is a key pathway involved in the survival, growth, and metabolic stability of tumor cells [67, 68]. As shown in Figures 4(e) and 4(f), the phosphorylation levels of AKT, GSK-3 β , and β -catenin were downregulated in the HA-ADT group. The data suggest that HA-ADT induces apoptosis via suppressing the AKT/GSK-3 β / β -catenin pathway in human HCC cells.

3.4. HA-ADT Decreases Autophagy of Human HCC Cells by Inhibiting the TGF- β /Smad2/3 Signaling Pathway. The role of autophagy in the development of cancer is extremely complex [69, 70]. Autophagy is a conservative catabolic process, which plays a dual role in regulating cell growth [71, 72]. Autophagy is an important mechanism by which cellular material is transferred to lysosome for degradation, thus providing energy and allowing the transformation of cellular components [70, 73, 74]. Beclin-1, LC3, and p62 are considered as specific autophagic markers [74]. As shown in Figures 5(a) and 5(b), the expressions of LC3 and beclin-1 in HA-ADT group were lower than those in the control, NaHS, and GYY4137 group, while the expression level of p62 exhibited the opposite trend. TGF- β plays an important role in cell homeostasis, fibrosis, angiogenesis, carcinogenesis, and differentiation. TGF- β can reduce apoptosis by inducing autophagy [75]. It has been shown that Smad2/3 is also involved in autophagy [76]. As shown in Figures 5(c) and

5(d), the expression levels of p-Smad2/3 and TGF- β in the HA-ADT group were lower than those in the control, NaHS, and GYY4137 group. These results indicate that HA-ADT can inhibit autophagy in human HCC cells via the TGF- β /Smad2/3 pathway.

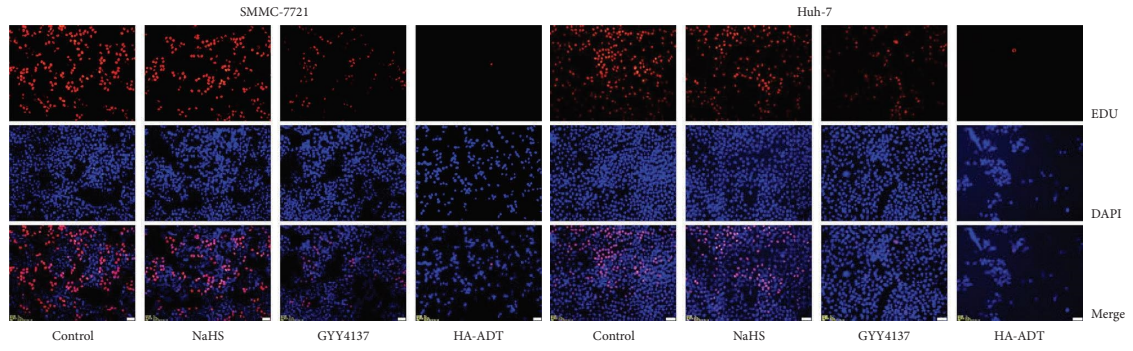
3.5. HA-ADT Suppresses the Growth of Human HCC Xenografted Tumors. SMMC-7721 and Huh-7 HCC cells have been successfully used to establish the subcutaneous xenograft models [77, 78]. Compared with the control, NaHS, and GYY4137 group, HA-ADT dramatically suppressed the growth of xenografted tumors (Figures 6(a)–6(e)). In addition, there was no significant difference in body weight between each group (Figures 6(f) and 6(g)). The expression levels of CD31, Ki67, p21, cleaved cas-3, and beclin-1 were further detected by IHC. As shown in Figure 7, the expression levels of CD31, Ki67, and beclin-1 in HA-ADT group were decreased, while p21 and cleaved cas-3 levels were increased in the HA-ADT group. These data demonstrate that HA-ADT can effectively suppress human HCC xenograft tumor growth by promoting apoptosis and reducing autophagy.

4. Discussion

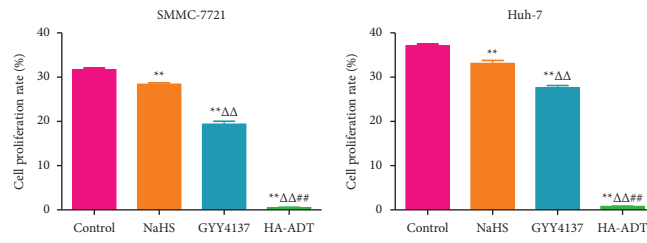
At present, H₂S is considered the third gaseous transmitter after CO and NO. H₂S is involved in many physiological and pathological processes in the human body [21–23, 79]. HA and its derivatives have the characteristics of plasticity, nonimmunogenicity, and good biocompatibility, which are widely adopted in the biomedical field, such as tissue engineering and drug delivery [39–41]. ADT is a methyl derivative of ADT-OH, which is a common H₂S donor [42, 79]. In the present study, HA-ADT was synthesized by chemical reaction as previously described [53].

Liver cancer is one of the leading causes of cancer death in the world [1–4]. Liver cancer is difficult to diagnose in the early stage, which will result in the death of patients. In addition, there are few effective treatments for patients with advanced liver cancer [3, 6, 13]. Thus, it is urgent to explore novel drugs to prevent and treat liver cancer. It has been revealed that 25–100 μ M-NaHS promotes the growth of HCC cells and blood vessel formation, while 800–1000 μ M-NaHS can inhibit angiogenesis and HCC growth [52]. Another study suggests that GYY4137 exhibits potent anti-HCC activity by blocking the signal transducer and activator of transcription 3 pathway [80]. In this study, we examined the roles of HA-ADT in the growth, migration, invasion, and cell cycle of human HCC cells. The results showed that HA-ADT was more effective than both NaHS and GYY4137 in inhibiting the survival, proliferation, migration, invasion, and cell cycle progression of human HCC cells. These results suggest that HA-ADT plays an effective role in inhibiting the development and progression of human HCC cells.

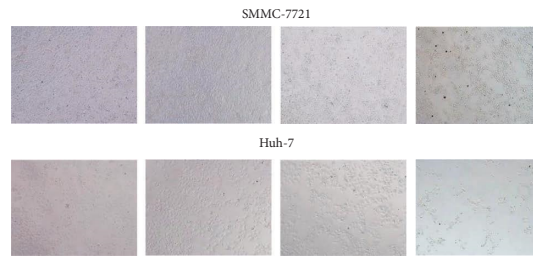
Apoptosis, a form of programmed cell death, is evolutionarily conserved and plays a key role in the homeostasis and development of mammalian tissues [81].



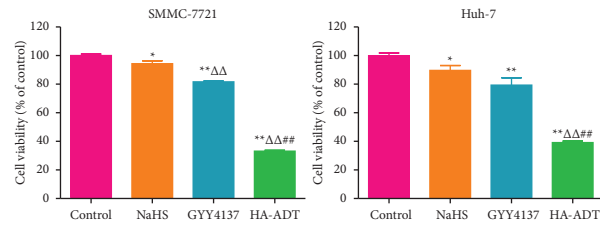
(a)



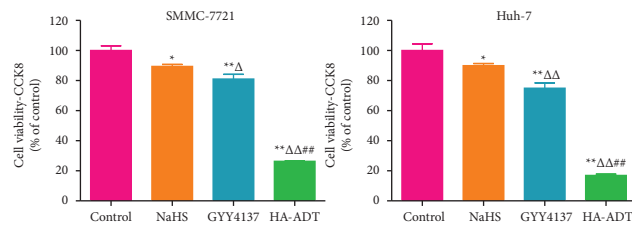
(b)



(c)



(d)



(e)

FIGURE 1: Continued.

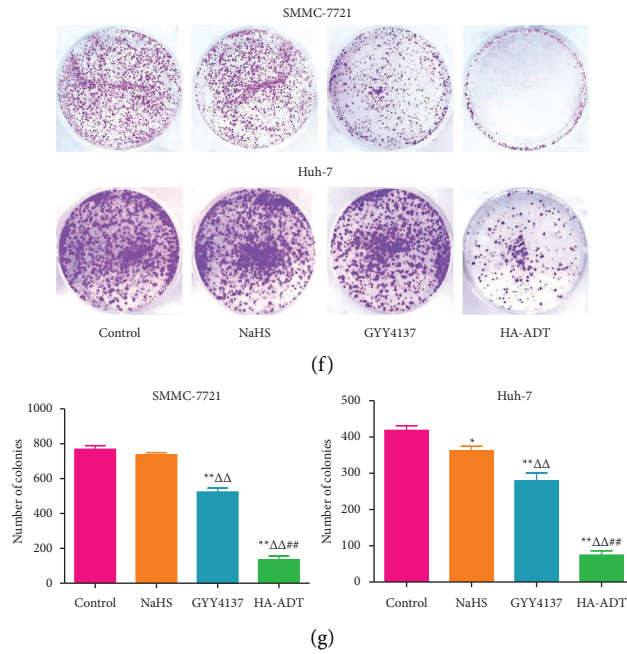


FIGURE 1: Effects of HA-ADT on proliferative ability and cell viability of human HCC cells. (a) EdU assay was adopted to determine DNA replication activity (original magnification, 100x). (b) Cell proliferation rate was calculated. (c) Phase contrast microscopy of Huh-7 and SMMC-7721 cells (original magnification, 100x). (d, e) Cell viability was measured by MTT and CCK8 assays. Cell viability in the control group was considered to be 100%. (f) The cells were treated for 2 weeks and then the clonogenic ability was detected. (g) The number of colonies was calculated. All data are shown as the mean \pm SEM of three independent experiments; * $P < 0.05$, ** $P < 0.01$ vs. control group; $\Delta P < 0.05$, $\Delta\Delta P < 0.01$ vs. NaHS group; ## $P < 0.01$ vs. GYY4137 group.

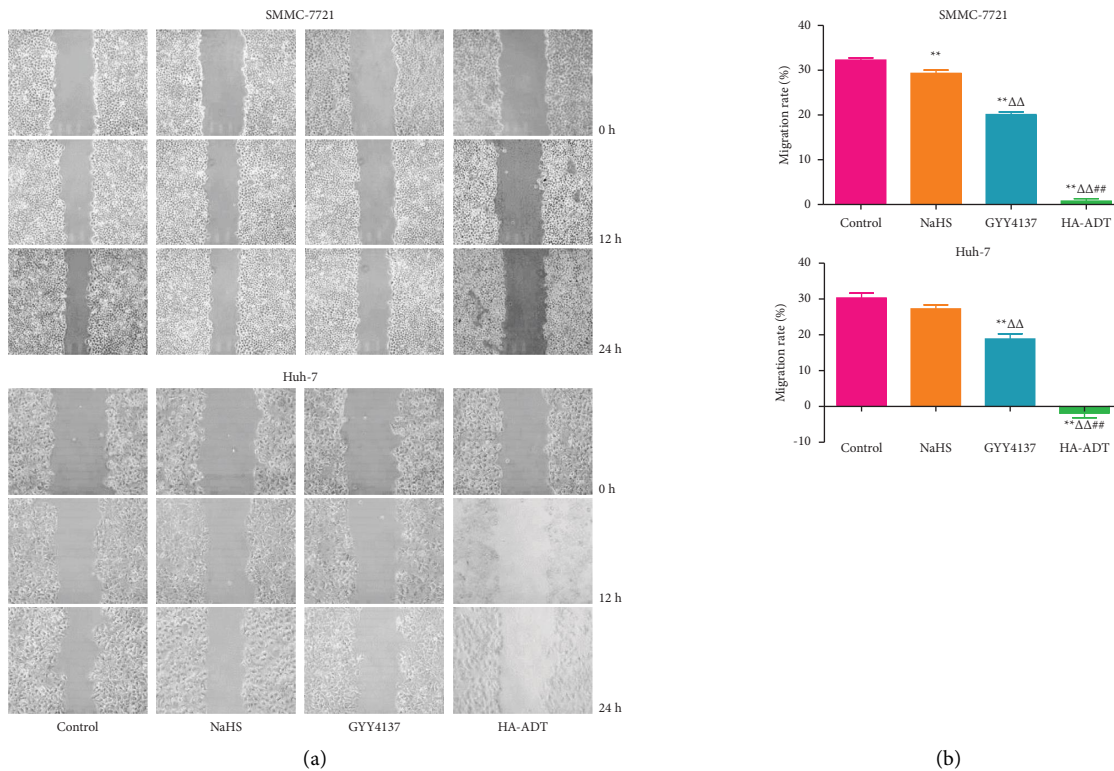


FIGURE 2: Continued.

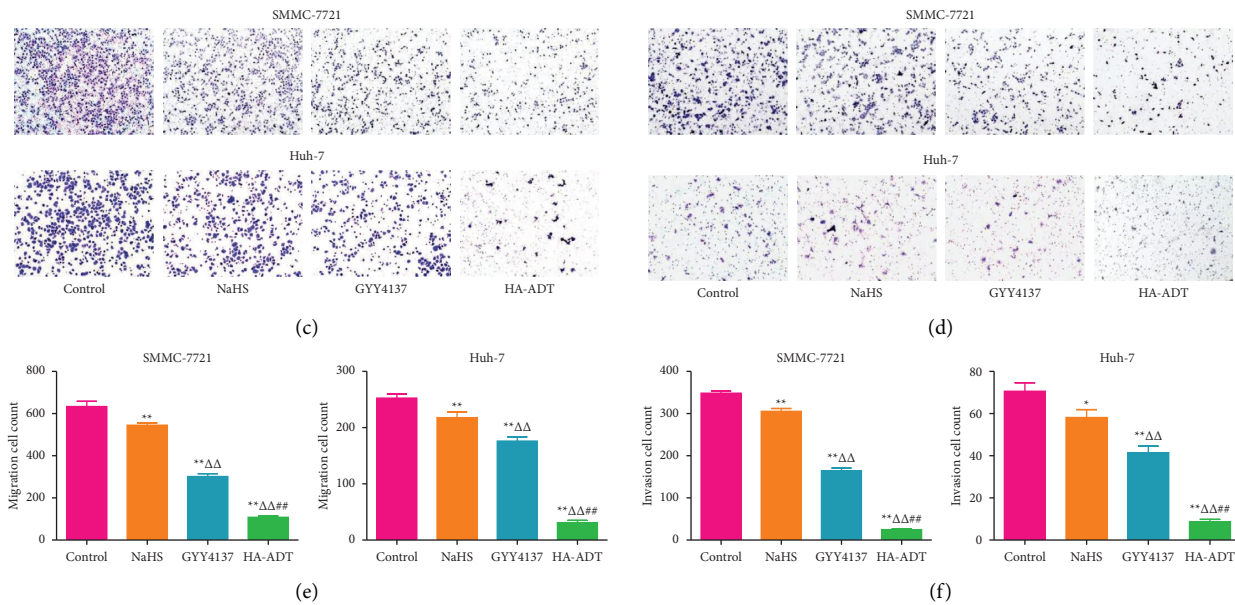


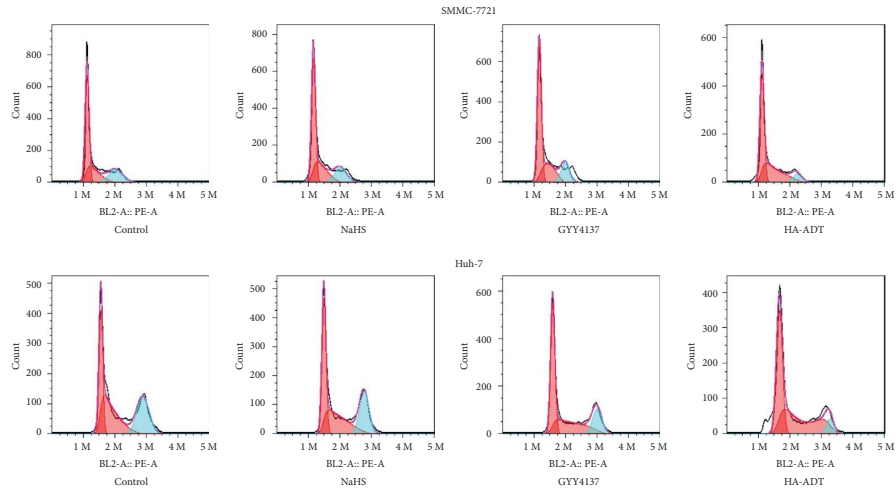
FIGURE 2: Effects of HA-ADT on the migrative and invasive capacities of human HCC cells. (a) Wound-healing assay was performed to determine cell migration (original magnification, 100x). (b) The migration rate was determined. (c, d) Transwell assay was carried out to evaluate the migrative and invasive abilities of human HCC cells (original magnification, 200x). (e, f) The numbers of the migrative and invasive cells were determined. All data are shown as the mean \pm SEM of three independent experiments; * $P < 0.05$, ** $P < 0.01$ vs. control group; $\Delta\Delta P < 0.01$ vs. NaHS group; ## $P < 0.01$ vs. GYY4137 group.

Apoptotic pathways can be divided into two categories: mitochondria-mediated intrinsic pathway and death receptor-mediated extrinsic pathway [82]. Bcl-2 family proteins are pivotal members in the process of apoptosis [53]. Caspases play key roles in apoptotic signaling pathways [83]. Caspases can be activated by many apoptotic stimuli and PARP is cleaved by cleaved caspase-3, resulting in the occurrence of apoptosis [53, 84]. It has been shown that NaHS effectively decreases the growth of C6 glioma cells by inducing caspase-dependent apoptosis [85]. Furthermore, GYY4137 could induce apoptosis in HCC cells by increasing the levels of cleaved cas-9, cas-3 and PARP cleavage [80]. Similarly, our results indicated that HA-ADT can promote apoptosis in HCC cells by up-regulating the levels of cleaved cas-3, 9, and cleaved PARP, indicating the activation of mitochondrial apoptosis. The AKT/GSK-3 β / β -catenin pathway is involved in a number of hallmarks of cancer, such as tumor grade and lympho-node metastasis [67, 68, 86]. It has been reported that the AKT pathway is involved in HCC growth and metastasis [68]. In addition, GSK-3 β plays a key role in the phosphorylation/degradation of β -catenin in the AKT/GSK-3 β / β -catenin pathway [68]. The results suggested that HA-ADT could reduce the expressions of p-AKT, p-GSK-3 β , and p- β -catenin in human liver cancer cells. The current research suggests that HA-ADT can inhibit the growth of human HCC cells by inducing apoptosis via inhibition of the AKT/GSK-3 β / β -catenin signaling pathway.

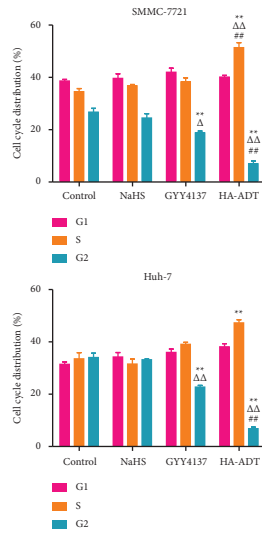
Autophagy could be neutral, tumor-promoting, or tumor-suppressive in different contexts in cancer cells [87]. A recent study has shown that diallyl trisulfide, a characterized H₂S

donor, inhibits the proliferation of urothelial carcinoma cells by promoting apoptosis and inducing autophagy [88]. Our previous study has demonstrated that HA-ADT could suppress the progression of esophageal squamous cell carcinoma via apoptosis promotion and autophagy inhibition [89]. Similarly, in the present study, our data showed that HA-ADT significantly reduced the autophagic level when compared to the control, NaHS, and GYY4137 group. It has been reported that the TGF- β pathway can activate autophagy in many human cancer cells, suggesting that induction of autophagy is a novel biological function of TGF- β [90]. Furthermore, as canonical effectors of TGF- β signaling, Smad2/3 are involved in the process of autophagy [91]. Moreover, another study suggests that specificity protein 1-mediated serine/threonine kinase 39 upregulation promotes the proliferation, migration, and invasion of HCC cells by activating the TGF- β 1/Smad2/3 pathway [47]. Our data indicated that HA-ADT decreased the expressions of p-Smad2/3 and TGF- β compared with the control, NaHS, and GYY4137 group. These findings indicate that HA-ADT can inhibit autophagy in human HCC cells through the TGF- β /Smad2/3 signaling pathway.

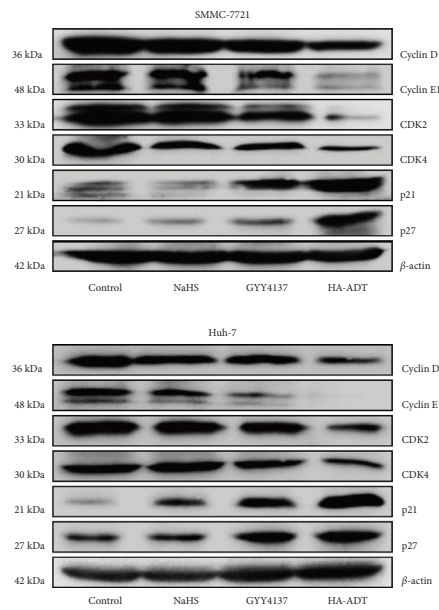
Recent studies suggest that SMMC-7721 and Huh-7 cells have been widely adopted to establish the xenograft tumor models [77, 78]. Therefore, we studied the role of HA-ADT in the growth of HCC xenograft tumor. We observed that HA-ADT exerted more inhibitory effects on HCC xenograft tumor growth than the control, NaHS, and GYY4137 group. Furthermore, there was no obvious change in the body weight in each group. Similar to the *in vitro* findings, our data suggested that the expressions of Ki67, CD31, and beclin-1 were decreased in HA-ADT group. The levels of p21 and cleaved cas-3 in the HA-ADT group were significantly higher than those in the



(a)



(b)



(c)

FIGURE 3: Continued.

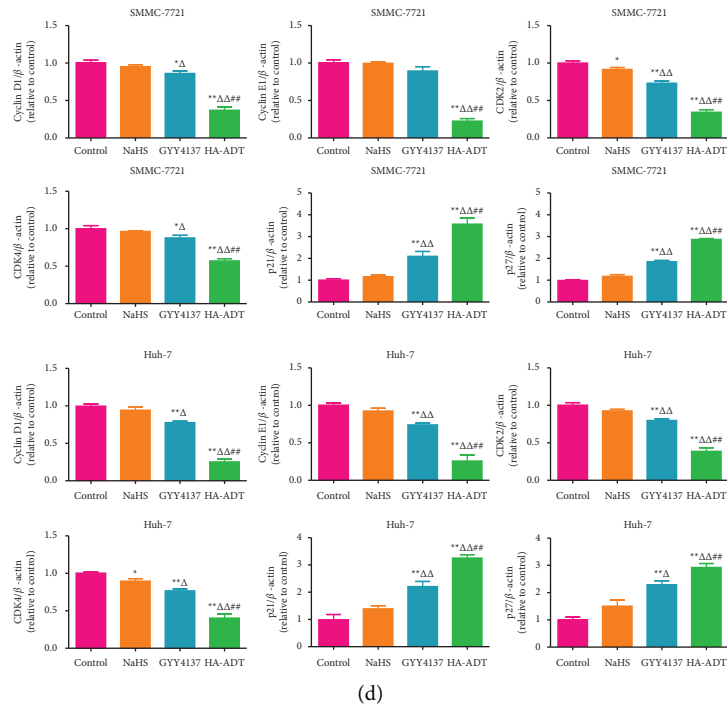


FIGURE 3: Effects of HA-ADT on the cell cycle of human HCC cells. (a) Cell cycle distribution was detected by flow cytometry. (b) The results of cell cycle distribution were analyzed. (c) The expression levels of cyclin D1/E1, CDK2/4, p21, and p27 were detected. β -actin was adopted as the internal control. (d) The band density was analyzed. All data are shown as the mean \pm SEM of three independent experiments; * $P < 0.05$, ** $P < 0.01$ vs. control group; $\Delta P < 0.05$, $\Delta\Delta P < 0.01$ vs. NaHS group; ## $P < 0.01$ vs. GYY4137 group.

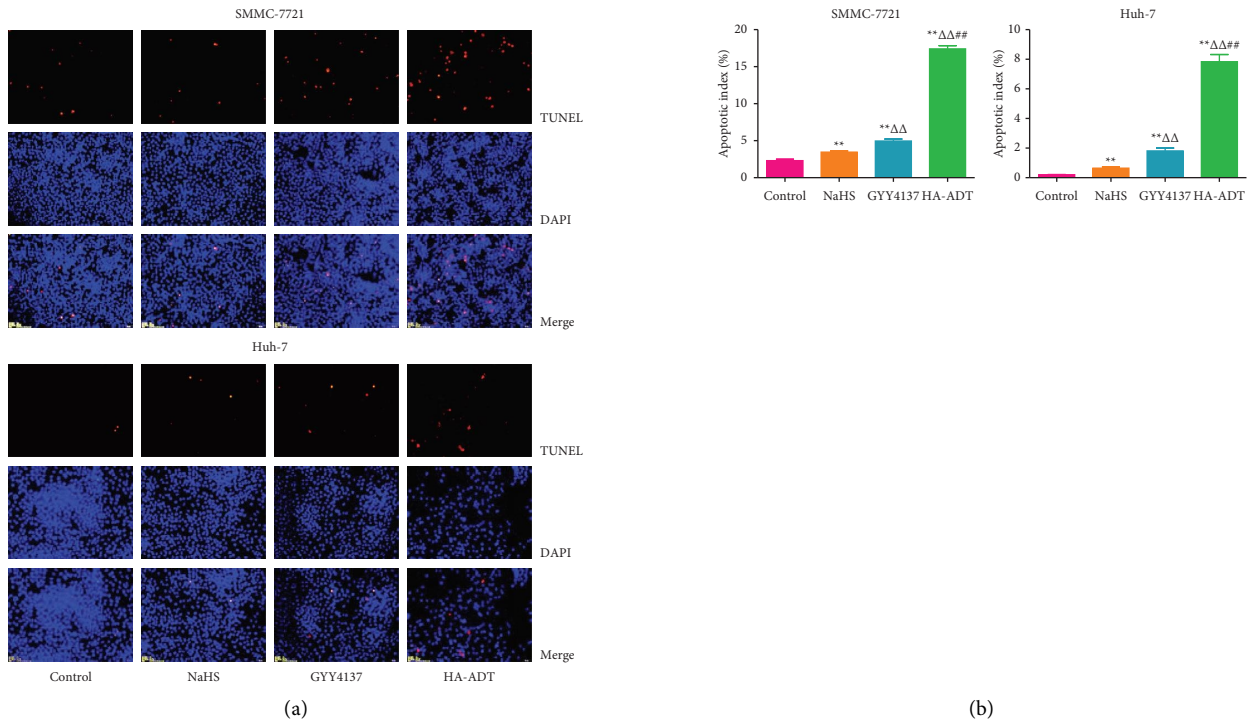


FIGURE 4: Continued.

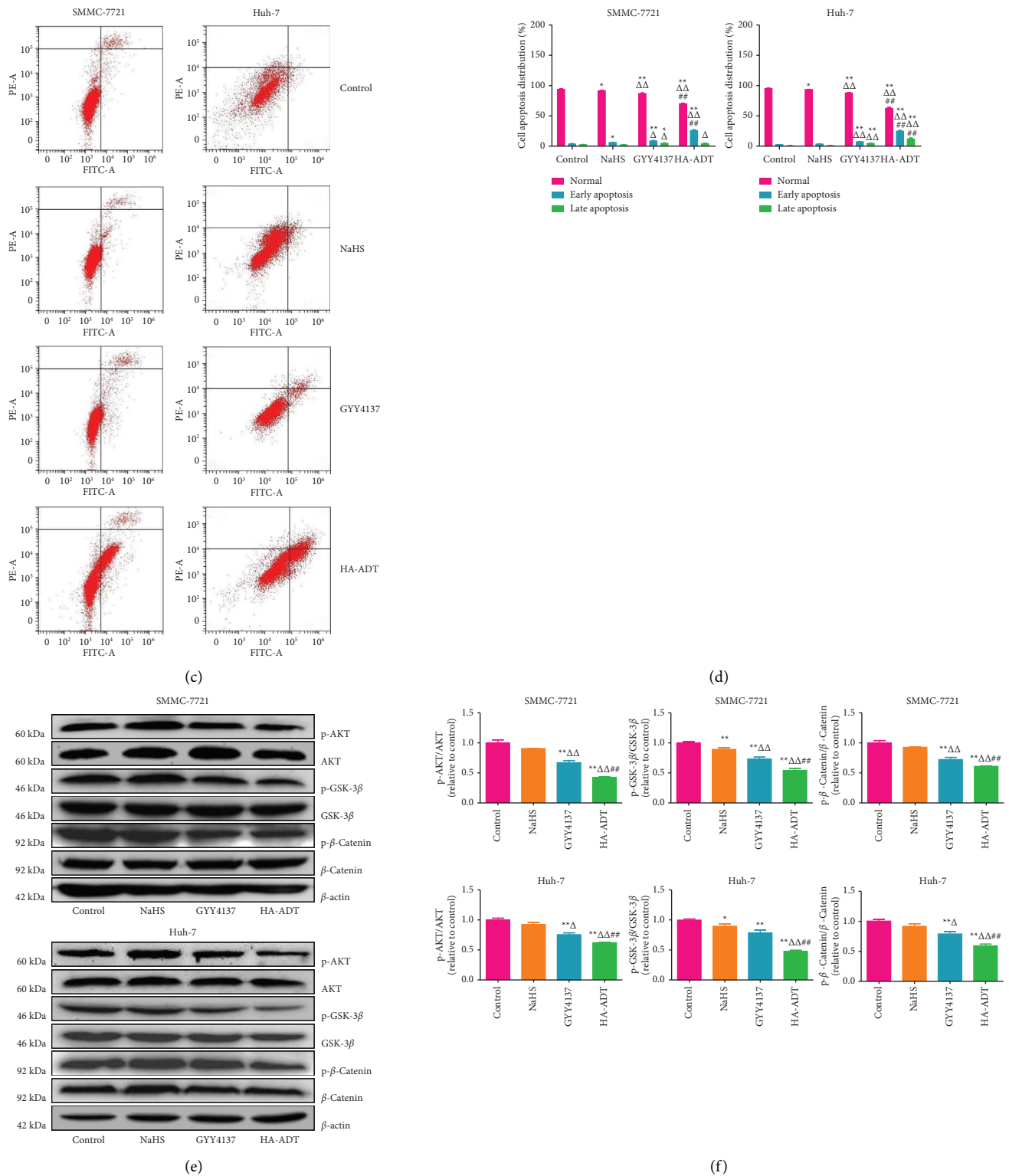


FIGURE 4: Effects of HA-ADT on the apoptotic level and AKT/GSK-3β/β-catenin pathway in human HCC cells. (a) TUNEL staining was used to detect the apoptotic level (original magnification, 100x). (b) The apoptotic index was counted as the ratio of TUNEL positive cells to total cells. (c) Flow cytometry assay was adopted to detect apoptosis. (d) Cell apoptosis distribution was analyzed. (e) Western blotting was used to determine the protein levels of AKT, p-AKT, GSK-3β, p-GSK-3β, β-catenin, and p-β-catenin. β-actin was adopted as the internal control. (f) The density was analyzed. All data are shown as the mean ± SEM of three independent experiments; **P* < 0.05, ***P* < 0.01 vs. control group; Δ*P* < 0.05, ΔΔ*P* < 0.01 vs. NaHS group; ##*P* < 0.01 vs. GYY4137 group.

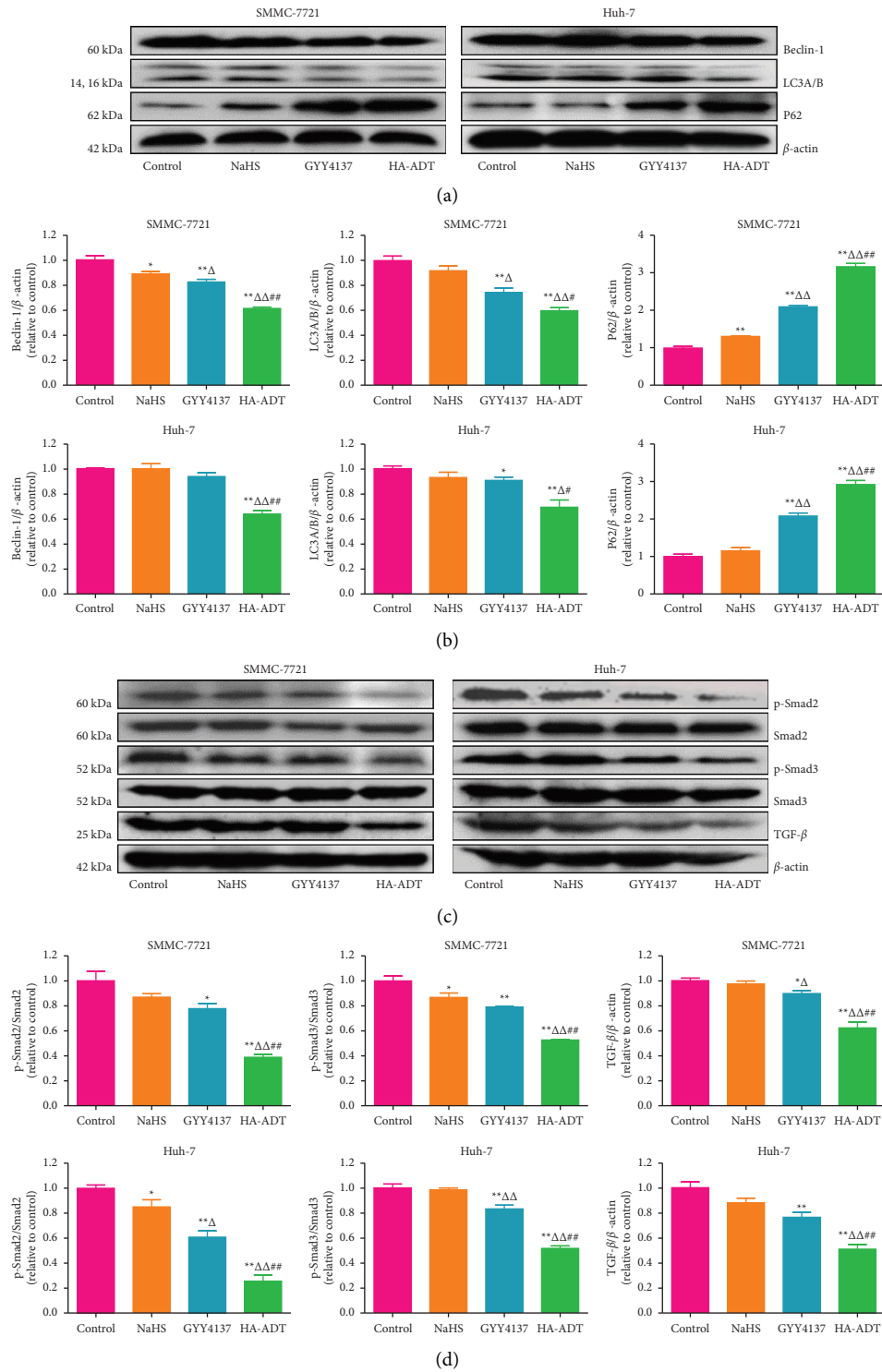


FIGURE 5: Effects of HA-ADT on the autophagic level and TGF- β /Smad2/3 signaling pathway in human HCC cells. (a) The protein levels of beclin-1, LC3A/B, and p62 were detected by western blotting. β -actin was adopted as the internal control. (b) The band density was analyzed. (c) The protein levels of p-Smad2, Smad2, p-Smad3, Smad3, and TGF- β were detected by western blotting. β -actin was adopted as the internal control. (d) The band density was analyzed. All data are shown as the mean \pm SEM of three independent experiments; * $P < 0.05$, ** $P < 0.01$ vs. control group; $\Delta P < 0.05$, $\Delta\Delta P < 0.01$ vs. NaHS group; # $P < 0.05$, ## $P < 0.01$ vs. GYY4137 group.

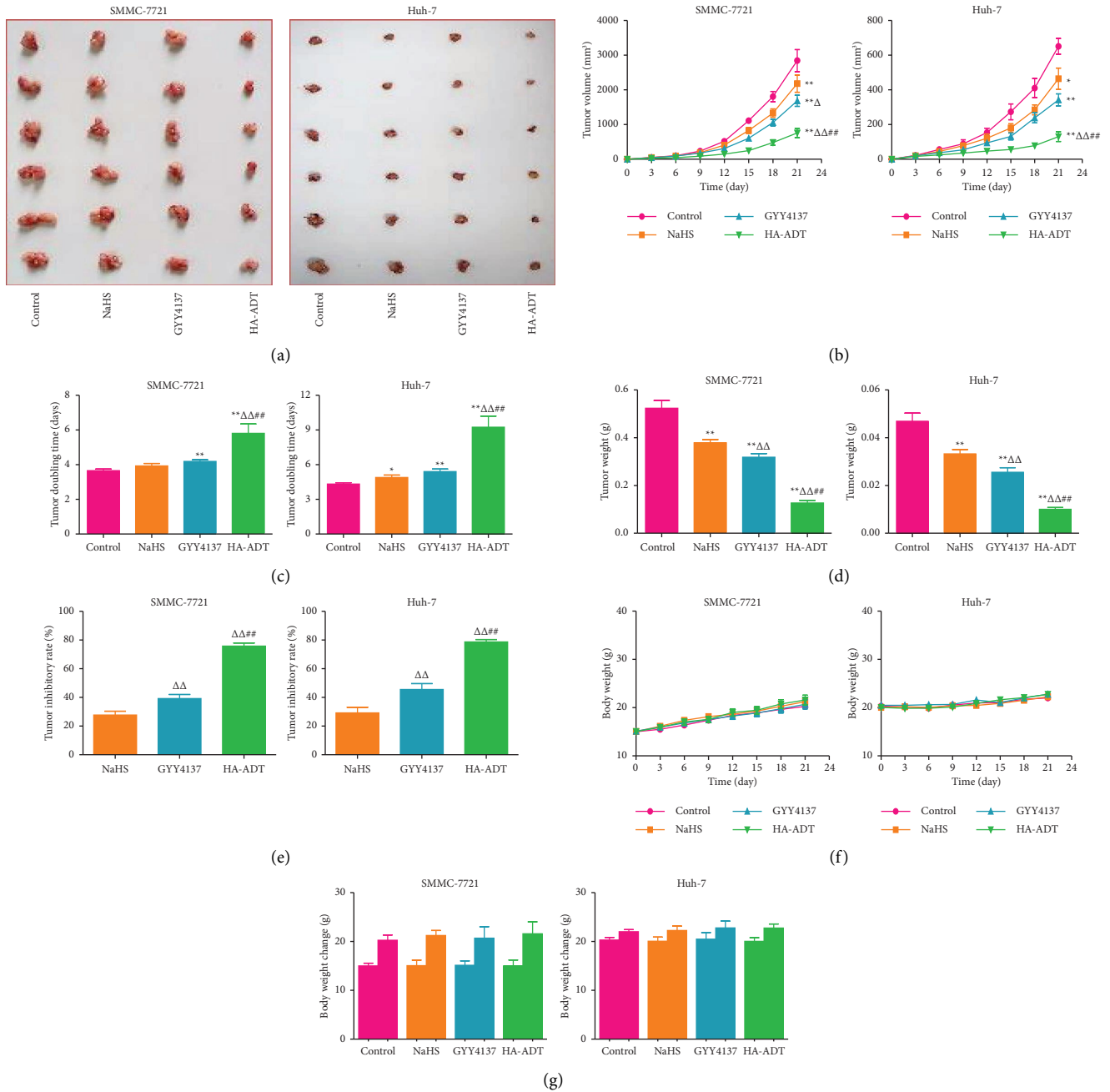


FIGURE 6: Effects of HA-ADT on human HCC xenograft tumor growth. (a) Representative xenograft tumors of each group were shown. (b, c) The tumor volume and TVDT were determined. (d, e) The tumor weight and tumor inhibitory rate were measured. (f, g) The body weight change curve and the body weights of mice (day 0 and day 21) were calculated. All data are presented as the mean ± SEM ($n = 6$); * $P < 0.05$, ** $P < 0.01$ vs. control group; $\Delta P < 0.05$, $\Delta\Delta P < 0.01$ vs. NaHS group; ## $P < 0.01$ vs. GYY4137 group.

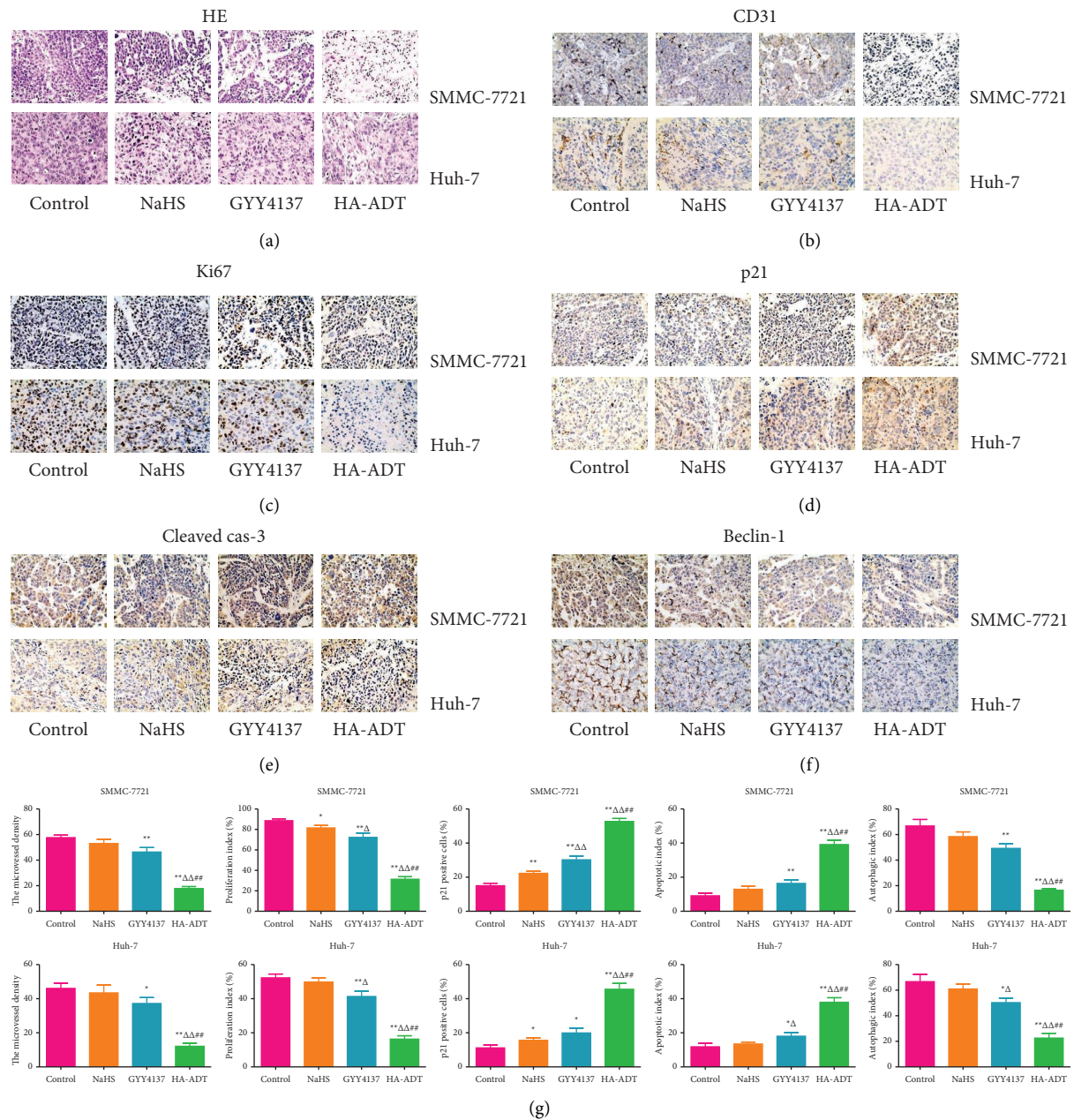


FIGURE 7: Effects of HA-ADT on MVD, PI, cell cycle, apoptosis, and autophagy of human HCC xenograft tumors. (a–f) Representative photographs of HE staining, and IHC staining with anti-CD31, anti-Ki67, anti-p21, anti-cleaved cas-3, and anti-beclin-1 antibodies in human HCC xenograft tumors (original magnification, 400x). (g) The MVD, proliferation index, p21 positive cells, apoptotic index, and autophagic index were determined. All data are presented as the mean \pm SEM ($n = 6$); * $P < 0.05$, ** $P < 0.01$ vs. control group; $\Delta P < 0.05$, $\Delta\Delta P < 0.01$ vs. NaHS group; ## $P < 0.01$ vs. GYY4137 group.

control, NaHS, and GYY4137 group. The data together indicate that HA-ADT can effectively inhibit the growth of human HCC xenograft tumors.

In sum, HA-ADT can suppress the proliferation, migration and invasion of human HCC cells via inhibition of the AKT/GSK-3 β / β -catenin and TGF- β /Smad2/3 signaling pathways. HA-ADT might be considered as a promising anticancer candidate for the treatment of HCC.

Data Availability

All data generated or analyzed in this study are included in this article.

Conflicts of Interest

The authors declare that they have no conflicts of interest.

Authors' Contributions

D.D.W., X.J.Z., and J.C. participated in the conception and design of the experiments. S.F.D., M.M.Z., Q. D., B.Y., W.L., X.Z., H.L.Y., S.H.Z., and N.H.K. carried out the experiments and analyzed the data. D.D.W. and S.F.D. prepared the manuscript. All authors read and approved the final manuscript. S.F.D and M.M.Z equally contributed to this study.

Acknowledgments

The study was supported by grants from the National Natural Science Foundation of China (no. 81802718), the Natural Science Foundation of Henan Province, China (no. 162300410044), the Foundation of Science & Technology Department of Henan Province, China (no. 202102310480), the Training Program for Young Backbone Teachers of Institutions of Higher Learning in Henan Province, China (no. 2020GGJS038), and the Science Foundation for Young Talents of Henan University College of Medicine, China (no. 2019013).

Supplementary Materials

Figure S1: Effects of HA-ADT on the expression levels of mitochondrial apoptosis-related proteins in human HCC cells. (a) Western blotting was used to detect the expressions of Bcl-2, Bax, Bcl-xl, Bad, cleaved cas-3, 9, and cleaved PARP in SMMC-7721 and Huh-7 cells. β -actin was adopted as the internal control. (b) The band density was analyzed. The Bax/Bcl-2 and Bad/Bcl-xl ratios were calculated. All data are shown as the mean \pm SEM of three independent experiments; * $P < 0.05$, ** $P < 0.01$ vs. control group; $\triangle P < 0.05$, $\triangle\triangle P < 0.01$ vs. NaHS group; ### $P < 0.01$ vs. GYY4137 group. (Supplementary Materials)

References

- [1] X. Ma, Y. T. Tan, Y. Yang et al., "Pre-diagnostic urinary 15-F_{2t}-isopros tane level and liver cancer risk: results from the Shanghai Women's and Men's Health Studies," *International Journal of Cancer*, vol. 143, no. 8, pp. 1896–1903, 2018.
- [2] D. Maucort-Boulch, C. de Martel, S. Franceschi, and M. Plummer, "Fraction and incidence of liver cancer attributable to hepatitis B and C viruses worldwide," *International Journal of Cancer*, vol. 142, no. 12, pp. 2471–2477, 2018.
- [3] J. Fu and H. Wang, "Precision diagnosis and treatment of liver cancer in China," *Cancer Letters*, vol. 412, pp. 283–288, 2018.
- [4] Z. Cheng, Z. Lei, P. Yang et al., "Long non-coding RNA THOR promotes liver cancer stem cells expansion via β -catenin pathway," *Gene*, vol. 684, pp. 95–103, 2019.
- [5] L. Li and H. Wang, "Heterogeneity of liver cancer and personalized therapy," *Cancer Letters*, vol. 379, no. 2, pp. 191–197, 2016.
- [6] Z. Cheng, X. Li, and J. Ding, "Characteristics of liver cancer stem cells and clinical correlations," *Cancer Letters*, vol. 379, no. 2, pp. 230–238, 2016.
- [7] L. Gailhouse, L. C. Liew, K. Yasukawa et al., "Differentiation therapy by epigenetic reconditioning exerts antitumor effects on liver cancer cells," *Molecular Therapy*, vol. 26, no. 7, pp. 1840–1854, 2018.
- [8] Y. Zhou, Y. Li, T. Zhou, J. Zheng, S. Li, and H. B. Li, "Dietary natural products for prevention and treatment of liver cancer," *Nutrients*, vol. 8, no. 3, p. 156, 2016.
- [9] T. W. Kensler, G. S. Qian, J. G. Chen, and J. D. Groopman, "Translational strategies for cancer prevention in liver," *Nature Reviews Cancer*, vol. 3, no. 5, pp. 321–329, 2003.
- [10] A. Marengo, C. Rosso, and E. Bugianesi, "Liver cancer: connections with obesity, fatty liver, and cirrhosis," *Annual Review of Medicine*, vol. 67, no. 1, pp. 103–117, 2016.
- [11] H. Lv, G. Lv, Q. Han, W. Yang, and H. Wang, "Noncoding RNAs in liver cancer stem cells: the big impact of little things," *Cancer Letters*, vol. 418, pp. 51–63, 2018.
- [12] A. Samson, M. J. Bentham, K. Scott et al., "Oncolytic reovirus as a combined antiviral and anti-tumour agent for the treatment of liver cancer," *Gut*, vol. 67, no. 3, pp. 562–573, 2018.
- [13] G. A. Michelotti, M. V. Machado, and A. M. Diehl, "NAFLD, NASH and liver cancer," *Nature Reviews Gastroenterology & Hepatology*, vol. 10, no. 11, pp. 656–665, 2013.
- [14] X. Y. Duan, L. Zhang, J. G. Fan, and L. Qiao, "NAFLD leads to liver cancer: do we have sufficient evidence?" *Cancer Letters*, vol. 345, no. 2, pp. 230–234, 2014.
- [15] K. Nikolaou, M. Sarris, and I. Talianidis, "Molecular pathways: the complex roles of inflammation pathways in the development and treatment of liver cancer," *Clinical Cancer Research*, vol. 19, no. 11, pp. 2810–2816, 2013.
- [16] Y. Pang, C. Kartsonaki, I. Turnbull et al., "Diabetes, plasma glucose, and incidence of fatty liver, cirrhosis, and liver cancer: a prospective study of 0.5 million people," *Hepatology*, vol. 68, no. 4, pp. 1308–1318, 2018.
- [17] X. Liu, A. Baecker, M. Wu et al., "Interaction between tobacco smoking and hepatitis B virus infection on the risk of liver cancer in a Chinese population," *International Journal of Cancer*, vol. 142, no. 8, pp. 1560–1567, 2018.
- [18] H. Nakagawa, M. Fujita, and A. Fujimoto, "Genome sequencing analysis of liver cancer for precision medicine," *Seminars in Cancer Biology*, vol. 55, pp. 120–127, 2019.
- [19] C. Yang, W. C. Cai, Z. T. Dong et al., "IncARSR promotes liver cancer stem cells expansion via STAT3 pathway," *Gene*, vol. 687, pp. 73–81, 2019.
- [20] J. Bruix, K. H. Han, G. Gores, J. M. Llovet, and V. Mazzaferro, "Liver cancer: approaching a personalized care," *Journal of Hepatology*, vol. 62, no. 1, pp. S144–S156, 2015.
- [21] K. Suzuki, M. Sagara, C. Aoki, S. Tanaka, and Y. Aso, "Clinical implication of plasma hydrogen sulfide levels in Japanese patients with type 2 diabetes," *Internal Medicine*, vol. 56, no. 1, pp. 17–21, 2017.
- [22] M. Li, C. Xu, J. Shi et al., "Fatty acids promote fatty liver disease via the dysregulation of 3-mercaptopyruvate sulfurtransferase/hydrogen sulfide pathway," *Gut*, vol. 67, no. 12, pp. 2169–2180, 2018.
- [23] S. Wang, X. Liu, and M. Zhang, "Reduction of amminerenium(III) by sulfide enables in vivo electrochemical monitoring of free endogenous hydrogen sulfide," *Analytical Chemistry*, vol. 89, no. 10, pp. 5382–5388, 2017.
- [24] Z. L. Luo, J. D. Ren, Z. Huang et al., "The role of exogenous hydrogen sulfide in free fatty acids induced inflammation in macrophages," *Cellular Physiology and Biochemistry*, vol. 42, no. 4, pp. 1635–1644, 2017.
- [25] P. Narne, V. Pandey, and P. B. Phanithi, "Role of nitric oxide and hydrogen sulfide in ischemic stroke and the emergent epigenetic underpinnings," *Molecular Neurobiology*, vol. 56, no. 3, pp. 1749–1769, 2019.

- [26] M. D. Wetzel and J. C. Wenke, "Mechanisms by which hydrogen sulfide attenuates muscle function following ischemia-reperfusion injury: effects on Akt signaling, mitochondrial function, and apoptosis," *Journal of Translational Medicine*, vol. 17, no. 1, p. 33, 2019.
- [27] M. Dulac, A. Melet, and E. Galardon, "Reversible detection and quantification of hydrogen sulfide by fluorescence using the hemoglobin I from *Lucina pectinata*," *ACS Sensors*, vol. 3, no. 10, pp. 2138–2144, 2018.
- [28] I. A. Szijártó, L. Markó, M. R. Filipovic et al., "Cystathionine γ -lyase-produced hydrogen sulfide controls endothelial NO bioavailability and blood pressure," *Hypertension*, vol. 71, no. 6, pp. 1210–1217, 2018.
- [29] Y. Zhao, H. A. Henthorn, and M. D. Pluth, "Kinetic insights into hydrogen sulfide delivery from caged-carbonyl sulfide isomeric donor platforms," *Journal of the American Chemical Society*, vol. 139, no. 45, pp. 16365–16376, 2017.
- [30] Z. Qiao, H. Zhang, K. Wang, and Y. Zhang, "A highly sensitive and responsive fluorescent probe based on 6-azide-chroman dye for detection and imaging of hydrogen sulfide in cells," *Talanta*, vol. 195, pp. 850–856, 2019.
- [31] Z. Huang, K. He, Z. Song et al., "Alleviation of heavy metal and silver nanoparticle toxicity and enhancement of their removal by hydrogen sulfide in *Phanerochaete chrysosporium*," *Chemosphere*, vol. 224, pp. 554–561, 2019.
- [32] F. Malagrino, K. Zuhra, L. Mascolo et al., "Hydrogen sulfide oxidation: adaptive changes in mitochondria of SW480 colorectal cancer cells upon exposure to hypoxia," *Oxidative Medicine and Cellular Longevity*, vol. 2019, Article ID 8102936, 11 pages, 2019.
- [33] M. Barton and M. R. Meyer, "HuR-ry up: how hydrogen sulfide protects against atherosclerosis," *Circulation*, vol. 139, no. 1, pp. 115–118, 2019.
- [34] Y. Luo, Y. Song, C. Zhu et al., "Visualization of endogenous hydrogen sulfide in living cells based on Au nanorods@silica enhanced fluorescence," *Analytica Chimica Acta*, vol. 1053, pp. 81–88, 2019.
- [35] S. Youssef, S. Zhang, and H. W. Ai, "A genetically encoded, ratiometric fluorescent biosensor for hydrogen sulfide," *ACS Sensors*, vol. 4, no. 6, pp. 1626–1632, 2019.
- [36] C. Hine, H. J. Kim, Y. Zhu et al., "Hypothalamic-pituitary Axis regulates hydrogen sulfide production," *Cell Metabolism*, vol. 25, no. 6, pp. 1320–1333.e5, 2017.
- [37] C. Rodrigues and S. S. Percival, "Immunomodulatory effects of glutathione, garlic derivatives, and hydrogen sulfide," *Nutrients*, vol. 11, no. 2, p. 295, 2019.
- [38] J. Behera, A. K. George, M. J. Voor, S. C. Tyagi, and N. Tyagi, "Hydrogen sulfide epigenetically mitigates bone loss through OPG/RANKL regulation during hyperhomocysteinemia in mice," *Bone*, vol. 114, pp. 90–108, 2018.
- [39] G. Huang and H. Huang, "Hyaluronic acid-based biopharmaceutical delivery and tumor-targeted drug delivery system," *Journal of Controlled Release*, vol. 278, pp. 122–126, 2018.
- [40] G. Huang and H. Huang, "Application of hyaluronic acid as carriers in drug delivery," *Drug Delivery*, vol. 25, no. 1, pp. 766–772, 2018.
- [41] A. Singh, M. Corvelli, S. A. Unterman, K. A. Wepasnick, P. McDonnell, and J. H. Elisseeff, "Enhanced lubrication on tissue and biomaterial surfaces through peptide-mediated binding of hyaluronic acid," *Nature Materials*, vol. 13, no. 10, pp. 988–995, 2014.
- [42] J. Jia, Y. Xiao, W. Wang et al., "Differential mechanisms underlying neuroprotection of hydrogen sulfide donors against oxidative stress," *Neurochemistry International*, vol. 62, no. 8, pp. 1072–1078, 2013.
- [43] L. A. Montoya and M. D. Pluth, "Organelle-Targeted H2S probes enable visualization of the subcellular distribution of H2S donors," *Analytical Chemistry*, vol. 88, no. 11, pp. 5769–5774, 2016.
- [44] M. Liao, H. Du, B. Wang, J. Huang, D. Huang, and G. Tong, "Anticancer effect of polyphyllin I in suppressing stem cell-like properties of hepatocellular carcinoma via the AKT/GSK-3 β / β -catenin signaling pathway," *Oxidative Medicine and Cellular Longevity*, vol. 2022, Article ID 4031008, 23 pages, 2022.
- [45] L. Zhuang, X. Wang, Z. Wang et al., "MicroRNA-23b functions as an oncogene and activates AKT/GSK3 β / β -catenin signaling by targeting ST7L in hepatocellular carcinoma," *Cell Death & Disease*, vol. 8, no. 5, Article ID e2804, 2017.
- [46] W. Zheng, M. Yao, M. Wu, J. Yang, D. Yao, and L. Wang, "Secretory clusterin promotes hepatocellular carcinoma progression by facilitating cancer stem cell properties via AKT/GSK-3 β / β -catenin axis," *Journal of Translational Medicine*, vol. 18, no. 1, p. 81, 2020.
- [47] J. Wang, Z. Fan, J. Li, J. Yang, X. Liu, and J. Cheng, "Transcription factor specificity protein 1-mediated Serine/threonine kinase 39 upregulation promotes the proliferation, migration, invasion and epithelial-mesenchymal transition of hepatocellular carcinoma cells by activating the transforming growth factor- β /Smad2/3 pathway," *Bioengineered*, vol. 12, no. 1, pp. 3566–3577, 2021.
- [48] M. Zhang, S. Zheng, C. Jing et al., "S100A11 promotes TGF- β 1-induced epithelial-mesenchymal transition through SMAD2/3 signaling pathway in intrahepatic cholangiocarcinoma," *Future Oncology*, vol. 14, no. 9, pp. 837–847, 2018.
- [49] J. Y. Shi, L. J. Ma, J. W. Zhang et al., "FOXP3 is a HCC suppressor gene and acts through regulating the TGF- β /Smad2/3 signaling pathway," *BMC Cancer*, vol. 17, no. 1, p. 648, 2017.
- [50] P. He, Z. Wang, B. Sheng et al., "Diallyl trisulfide regulates cell apoptosis and invasion in human osteosarcoma U2OS cells through regulating PI3K/AKT/GSK3 β signaling pathway," *Histology & Histopathology*, vol. 35, no. 12, pp. 1511–1520, 2020.
- [51] Y. W. Bai, M. J. Ye, D. L. Yang, M. P. Yu, C. F. Zhou, and T. Shen, "Hydrogen sulfide attenuates paraquat-induced epithelial-mesenchymal transition of human alveolar epithelial cells through regulating transforming growth factor- β 1/Smad2/3 signaling pathway," *Journal of Applied Toxicology*, vol. 39, no. 3, pp. 432–440, 2019.
- [52] D. Wu, M. Li, W. Tian et al., "Hydrogen sulfide acts as a double-edged sword in human hepatocellular carcinoma cells through EGFR/ERK/MMP-2 and PTEN/AKT signaling pathways," *Scientific Reports*, vol. 7, no. 1, p. 5134, 2017.
- [53] Q. Dong, B. Yang, J. G. Han et al., "A novel hydrogen sulfide-releasing donor, HA-ADT, suppresses the growth of human breast cancer cells through inhibiting the PI3K/AKT/mTOR and Ras/Raf/MEK/ERK signaling pathways," *Cancer Letters*, vol. 455, pp. 60–72, 2019.
- [54] G. Y. Zhang, D. Lu, S. F. Duan et al., "Hydrogen sulfide alleviates lipopolysaccharide-induced diaphragm dysfunction in rats by reducing apoptosis and inflammation through ROS/MAPK and TLR4/NF- κ B signaling pathways," *Oxidative Medicine and Cellular Longevity*, vol. 2018, Article ID 9647809, 15 pages, 2018.

- [55] A. Quarta, M. Amorin, M. J. Aldegunde et al., "Novel synthesis of platinum complexes and their intracellular delivery to tumor cells by means of magnetic nanoparticles," *Nanoscale*, vol. 11, no. 48, pp. 23482–23497, 2019.
- [56] D. Wu, P. Zhong, J. Wang, and H. Wang, "Exogenous hydrogen sulfide mitigates LPS + ATP-induced inflammation by inhibiting NLRP3 inflammasome activation and promoting autophagy in L02 cells," *Molecular and Cellular Biochemistry*, vol. 457, no. 1-2, pp. 145–156, 2019.
- [57] J. Zhang, H. Si, B. Li, X. Zhou, and J. Zhang, "Myrislignan exhibits activities against toxoplasma gondii RH strain by triggering mitochondrial dysfunction," *Frontiers in Microbiology*, vol. 10, p. 2152, 2019.
- [58] D. D. Wu, Y. R. Gao, T. Li et al., "PEST-containing nuclear protein mediates the proliferation, migration, and invasion of human neuroblastoma cells through MAPK and PI3K/AKT/mTOR signaling pathways," *BMC Cancer*, vol. 18, no. 1, p. 499, 2018.
- [59] D. Y. Wang, Y. Hong, Y. G. Chen et al., "PEST-containing nuclear protein regulates cell proliferation, migration, and invasion in lung adenocarcinoma," *Oncogenesis*, vol. 8, no. 3, p. 22, 2019.
- [60] E. K. Manesis, G. Giannoulis, P. Zoumboulis, I. Vafiadou, and S. J. Hadziyannis, "Treatment of hepatocellular carcinoma with combined suppression and inhibition of sex hormones: a randomized, controlled trial," *Hepatology*, vol. 21, no. 6, pp. 1535–1542, 1995.
- [61] D. Wu, J. Li, Q. Zhang et al., "Exogenous hydrogen sulfide regulates the growth of human thyroid carcinoma cells," *Oxidative Medicine and Cellular Longevity*, vol. 2019, Article ID 6927298, 18 pages, 2019.
- [62] P. Dong, H. Fu, L. Chen et al., "PCNP promotes ovarian cancer progression by accelerating β -catenin nuclear accumulation and triggering EMT transition," *Journal of Cellular and Molecular Medicine*, vol. 24, no. 14, pp. 8221–8235, 2020.
- [63] D. D. Wu, S. Y. Liu, Y. R. Gao et al., "Tumour necrosis factor- α -induced protein 8-like 2 is a novel regulator of proliferation, migration, and invasion in human rectal adenocarcinoma cells," *Journal of Cellular and Molecular Medicine*, vol. 23, no. 3, pp. 1698–1713, 2019.
- [64] J. S. Huang, C. M. Yang, J. S. Wang et al., "Caspase-3 expression in tumorigenesis and prognosis of buccal mucosa squamous cell carcinoma," *Oncotarget*, vol. 8, no. 48, pp. 84237–84247, 2017.
- [65] D. R. Green and F. Llambi, "Cell death signaling," *Cold Spring Harbor Perspectives in Biology*, vol. 7, no. 12, Article ID a006080, 2015.
- [66] P. Pitchakarn, S. Suzuki, K. Ogawa et al., "Induction of G1 arrest and apoptosis in androgen-dependent human prostate cancer by Kuguacin J, a triterpenoid from Momordica charantia leaf," *Cancer Letters*, vol. 306, no. 2, pp. 142–150, 2011.
- [67] C. Wang, H. Jin, N. Wang et al., "Gas6/Axl Axis contributes to chemoresistance and metastasis in breast cancer through akt/GSK-3 β / β -catenin signaling," *Theranostics*, vol. 6, no. 8, pp. 1205–1219, 2016.
- [68] Q. Xu, H. X. Xu, J. P. Li et al., "Growth differentiation factor 15 induces growth and metastasis of human liver cancer stem-like cells via AKT/GSK-3 β / β -catenin signaling," *Oncotarget*, vol. 8, no. 10, pp. 16972–16987, 2017.
- [69] H. Pan, Y. Wang, K. Na et al., "Autophagic flux disruption contributes to Ganoderma lucidum polysaccharide-induced apoptosis in human colorectal cancer cells via MAPK/ERK activation," *Cell Death & Disease*, vol. 10, no. 6, p. 456, 2019.
- [70] J. M. M. Levy, C. G. Towers, and A. Thorburn, "Targeting autophagy in cancer," *Nature Reviews Cancer*, vol. 17, no. 9, pp. 528–542, 2017.
- [71] J. Niu, T. Yan, W. Guo, W. Wang, and Z. Zhao, "Insight into the role of autophagy in osteosarcoma and its therapeutic implication," *Frontiers in Oncology*, vol. 9, p. 1232, 2019.
- [72] L. Wang, M. E. A. Howell, B. McPeak et al., "LIMD1 is induced by and required for LMP1 signaling, and protects EBV-transformed cells from DNA damage-induced cell death," *Oncotarget*, vol. 9, no. 5, pp. 6282–6297, 2017.
- [73] N. Mizushima and M. Komatsu, "Autophagy: renovation of cells and tissues," *Cell*, vol. 147, no. 4, pp. 728–741, 2011.
- [74] L. Tian, Z. Zhao, L. Xie, and J. Zhu, "MiR-361-5p suppresses chemoresistance of gastric cancer cells by targeting FOXM1 via the PI3K/Akt/mTOR pathway," *Oncotarget*, vol. 9, no. 4, pp. 4886–4896, 2017.
- [75] Y. Ding, J. K. Kim, S. I. Kim et al., "TGF- β 1 protects against mesangial cell apoptosis via induction of autophagy," *Journal of Biological Chemistry*, vol. 285, no. 48, pp. 37909–37919, 2010.
- [76] S. M. Pokharel, N. K. Shil, and S. Bose, "Autophagy, TGF- β , and SMAD-2/3 signaling regulates interferon- β response in respiratory syncytial virus infected macrophages," *Frontiers in Cellular and Infection Microbiology*, vol. 6, p. 174, 2016.
- [77] J. Liao, H. Jin, S. Li et al., "Apatinib potentiates irradiation effect via suppressing PI3K/AKT signaling pathway in hepatocellular carcinoma," *Journal of Experimental & Clinical Cancer Research*, vol. 38, no. 1, p. 454, 2019.
- [78] X. Zhang, T. Liu, Z. Li et al., "Hepatomas are exquisitely sensitive to pharmacologic ascorbate (P-Asch -)," *Theranostics*, vol. 9, no. 26, pp. 8109–8126, 2019.
- [79] Y. Liu, J. Li, H. Chen et al., "Magnet-activatable nanoliposomes as intracellular bubble microreactors to enhance drug delivery efficacy and burst cancer cells," *Nanoscale*, vol. 11, no. 40, pp. 18854–18865, 2019.
- [80] S. Lu, Y. Gao, X. Huang, and X. Wang, "GYY4137, a hydrogen sulfide (H₂S) donor, shows potent anti-hepatocellular carcinoma activity through blocking the STAT3 pathway," *International Journal of Oncology*, vol. 44, no. 4, pp. 1259–1267, 2014.
- [81] X. Cheng and J. E. Ferrell, "Apoptosis propagates through the cytoplasm as trigger waves," *Science*, vol. 361, no. 6402, pp. 607–612, 2018.
- [82] P. Zhang, Y. Zhang, K. Liu et al., "Ivermectin induces cell cycle arrest and apoptosis of HeLa cells via mitochondrial pathway," *Cell Proliferation*, vol. 52, no. 2, Article ID e12543, 2019.
- [83] Y. Bai, X. Liu, X. Qi et al., "PDIA6 modulates apoptosis and autophagy of non-small cell lung cancer cells via the MAP4K1/JNK signaling pathway," *EBioMedicine*, vol. 42, pp. 311–325, 2019.
- [84] H. Y. Hsu, T. Y. Lin, C. H. Hu, D. T. F. Shu, and M. K. Lu, "Fucoidan upregulates TLR4/CHOP-mediated caspase-3 and PARP activation to enhance cisplatin-induced cytotoxicity in human lung cancer cells," *Cancer Letters*, vol. 432, pp. 112–120, 2018.
- [85] L. Zhao, Y. Wang, Q. Yan, W. Lv, Y. Zhang, and S. He, "Exogenous hydrogen sulfide exhibits anti-cancer effects through p38 MAPK signaling pathway in C6 glioma cells," *Biological Chemistry*, vol. 396, no. 11, pp. 1247–1253, 2015.
- [86] J. Yu, X. Wang, Q. Lu et al., "Extracellular 5'-nucleotidase (CD73) promotes human breast cancer cells growth through AKT/GSK-3 β / β -catenin/cyclinD1 signaling pathway," *International Journal of Cancer*, vol. 142, no. 5, pp. 959–967, 2018.

- [87] R. Amaravadi, A. C. Kimmelman, and E. White, "Recent insights into the function of autophagy in cancer," *Genes & Development*, vol. 30, no. 17, pp. 1913–1930, 2016.
- [88] E. Panza, I. Bello, M. Smimmo et al., "Endogenous and exogenous hydrogen sulfide modulates urothelial bladder carcinoma development in human cell lines," *Biomedicine & Pharmacotherapy*, vol. 151, Article ID 113137, 2022.
- [89] S. F. Duan, M. M. Zhang, X. Zhang et al., "HA-ADT suppresses esophageal squamous cell carcinoma progression via apoptosis promotion and autophagy inhibition," *Experimental Cell Research*, vol. 420, no. 1, Article ID 113341, 2022.
- [90] K. Kiyono, H. I. Suzuki, H. Matsuyama et al., "Autophagy is activated by TGF-beta and potentiates TGF-beta-mediated growth inhibition in human hepatocellular carcinoma cells," *Cancer Research*, vol. 69, no. 23, pp. 8844–8852, 2009.
- [91] C. C. Pan, S. Kumar, N. Shah et al., "Endoglin regulation of Smad2 function mediates Beclin1 expression and endothelial autophagy," *Journal of Biological Chemistry*, vol. 290, no. 24, pp. 14884–14892, 2015.